Saturation broadening of laser-induced fluorescence from plasma ions

M. J. Goeckner,[a] J. Goree, and T. E. Sheridan[b]
Department of Physics and Astronomy, The University of Iowa, Iowa City, Iowa 52242

(Received 15 June 1992; accepted for publication 15 December 1992)

Saturation broadening is an obstacle in using laser-induced fluorescence as a plasma diagnostic. The Doppler-broadened line shape ideally yields the ion velocity distribution function, but at high laser power, saturation of the optical transition leads to additional undesirable line broadening. We test three different prescriptions for plasma experimentalists to avoid saturation broadening while maintaining a strong signal. Based on experiments in an argon plasma, and a semiclassical atomic physics simulation, we have identified the prescription that is the easiest to use and the least sensitive to the spatial profile of the laser beam. This procedure is to measure the laser intensity that leads to saturation on the peak of the spectral line, and then to reduce the intensity to 20% of the saturation level.

I. INTRODUCTION

Laser-induced fluorescence (LIF) is a nonperturbing, *in situ* plasma diagnostic that offers spatial and temporal resolution. With LIF one can measure ion velocity distributions,[1–4] electron densities and temperatures,[5,6] ion diffusion,[7,8] plasma waves,[9] electric fields,[10] and magnetic fields.[10] LIF can be used to detect ions or neutrals, of either atomic or molecular composition. A beam from a tunable laser is directed at a plasma, where it is absorbed on one spectral line, resulting in fluorescence on another line. The fluorescence is collected, and measured to determine the desired plasma parameter. When a narrow-bandwidth laser is used, the shape of the absorption spectral line can be measured; this is termed sub-Doppler LIF if the laser bandwidth is less than the Doppler-broadened linewidth. In this paper we investigate a practical problem that affects sub-Doppler LIF measurements of plasma ions.

First, we summarize how sub-Doppler measurements work. The laser excites to a higher state only those ions with a velocity satisfying the Doppler shift condition,

$$2\pi\Delta\nu=\mathbf{v}\cdot\mathbf{k}=v_{\|}\,k. \tag{1}$$

Here $\mathbf{k}$ is the incident laser photon wave vector, $\mathbf{v}$ is the ion velocity, $v_{\|}$ is the component of the ion velocity parallel to the direction of the laser beam, and $\Delta\nu$ is the difference between the laser frequency and the transition frequency of a stationary ion. The strength of the fluorescence indicates the number of ions satisfying the Doppler condition. The line shape is found by tuning the wavelength of a laser through the spectral line while measuring the fluorescence.[2–4] Ideally the Doppler-broadened line shape is the same shape as the ion velocity distribution function. From this one can calculate the temperature, average drift velocity, and density of the ions. Any nonthermal features in the distribution can also be detected. The ion temperature T_i for a Maxwellian distribution is determined from the line width $\Delta\nu_{\mathrm{FWHM}}$ by the simple relation[11]

$$T_i=\frac{\Delta\nu_{\mathrm{FWHM}}^2 M_i c^2}{2\nu_{01}^2\ln 2}. \tag{2}$$

Here T_i is in units of energy, M_i is the ion mass, c is the speed of light, ν_{01} is the central frequency of the transition, and $\Delta\nu_{\mathrm{FWHM}}$ is the full width at half maximum of the spectral line in units of frequency. Equation (2) is accurate if Doppler broadening is the only broadening mechanism in effect. The other mechanisms include the natural linewidth,[12] pressure broadening,[13] Stark broadening,[13,14] Stark splitting,[15] Zeeman splitting,[15] and saturation broadening.[11,16,17] If these are not avoided, Eq. (2) will give an erroneous large value for T_i, and any small nonthermal features in the distribution function will be obscured.

In this paper we address saturation broadening, which occurs at high laser intensities because of the finite bandwidth of a laser and because LIF is a nonlinear process. As has been shown elsewhere,[11,16,17] results obtained using lasers with wide bandwidths and high intensities are especially prone to error due to saturation broadening. It is avoided by reducing the laser intensity, which can sacrifice signal strength.[11,16,17]

To understand saturation broadening, first consider a single optical frequency ν. The signal increases linearly with intensity until the onset of saturation, as sketched in Fig. 1. When saturation occurs, the ions can no longer absorb additional photons, and the signal no longer increases with intensity. Now consider that a laser does not operate at just a single frequency, but instead has a finite bandwidth, as sketched in Fig. 2. Photons with frequencies at the peak of the laser spectrum will saturate the transition first. Increasing the laser intensity causes saturation over a broader range of frequencies, extending to the wings of the laser's spectrum. A strong fluorescence signal will then be observed, even when the central frequency of the laser is not tuned to the spectral line. When the line shape is measured by recording the signal versus central laser frequency, it will be broadened.

[a]Current address: Engineering Research Center for Plasma Aided Manufacturing, Room 101, 1410 Johnson Drive, University of Wisconsin, Madison, WI 53706-1806.
[b]Current address: Department of Physics, West Virginia University, Morgantown, WV 26506.

 0034-6748/93/040996-05$06.00

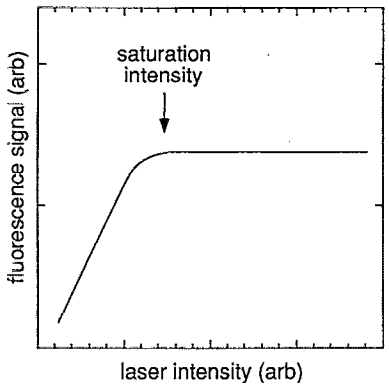

FIG. 1. Strength of the fluorescence signal as a function of laser intensity. This sketch (for a single laser frequency) illustrates how LIF is a nonlinear process at high intensities.

The aim of this paper is to identify and test quantitative techniques to avoid saturation broadening with the least possible loss of signal. We carried out experimental tests of the three techniques that were proposed in Ref. 11, which were based on atomic physics theory. Our experimental method is presented in Sec. II, and the theory is reviewed in Sec. III. In Sec. IV we test the three techniques. We sought a reliable method that requires no additional equipment, is simple to carry out, does not require extensive and time-consuming signal averaging, and is unaffected by influences out of the experimenter's control. One such influence is the spatial profile of the laser beam, which has a significant effect on the saturation broadening of a line shape.[18] We find that the best method is to tune the laser to the spectral line peak, measure the laser intensity that leads to saturation, and then reduce the power to 20% of that level.

II. EXPERIMENT

A. Apparatus

To best observe the effects of saturation broadening, we used a plasma with a very low ion temperature of 0.028 $\pm$0.007 eV. This was an argon discharge, powered by hot

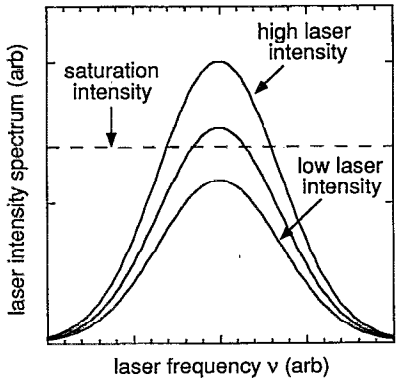

FIG. 2. Sketch of a laser's frequency spectrum. For low intensities, the laser will not saturate the probed transition. For higher intensity, the laser saturates the transition at the peak of the spectrum. If the intensity is further increased, the transition will be saturated at frequencies in the wings of the laser's spectrum.

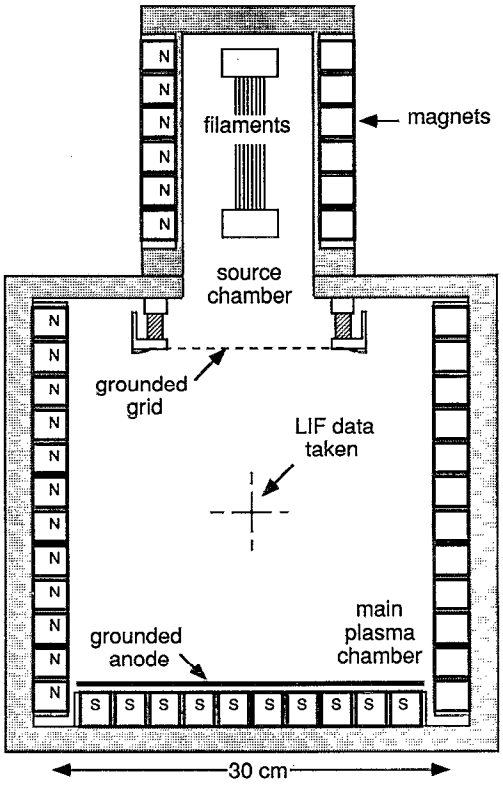

FIG. 3. Plasma chamber.

tungsten filaments and confined by a multidipole magnetic field.[19] The plasma chamber is sketched in Fig. 3. The vacuum vessel was divided into two sections, separated by a grid at ground potential. The filaments were housed in the upper chamber. Downstream was a larger 32-cm-diam main chamber where we made LIF measurements. The main chamber was made of black anodized aluminum to reduce scattered light, and it was fitted with Pyrex windows. The multidipole magnetic field was provided by 19 rows of 2.5-cm-long, 2.2-cm-diam ceramic magnets. On the magnet surface, the field is 1.05$\pm$0.19 kG. The field quickly diminishes away from the magnet surface; in the center of the main chamber, it is less than 7 G. Further details of this multidipole device are found in Ref. 4.

The plasma parameters were 0.050 Pa neutral argon pressure, 40.0 V discharge voltage, and 1.0 A discharge current. Using LIF, we found that $T_i = 0.028 \pm 0.007$ eV along the direction of the laser beam, measured in the center of this discharge.[4] The plasma at this location was characterized by an 1.5×10^{15} m^{-3} electron density, 1 eV electron temperature, and 1.5 V plasma potential.

We carried out LIF measurements using the 611.492 nm Ar^+ transition, which is popular amongst plasma experimentalists. Fluorescence was detected at 460.957 nm. This corresponds to probing the $3d'\ ^2G_{9/2} \leftrightarrow 4p'\ ^2F^0_{7/2} \rightarrow 4s'\ ^2D_{5/2}$ transition, as illustrated in Fig. 4. All of these states are electronically excited. The probed state is metastable, so that it will have enough population to be detectable. The results presented below would probably be the same, had we chosen another Ar^+ metastable state.

We used a YAG-pumped tunable dye laser (Lumonics

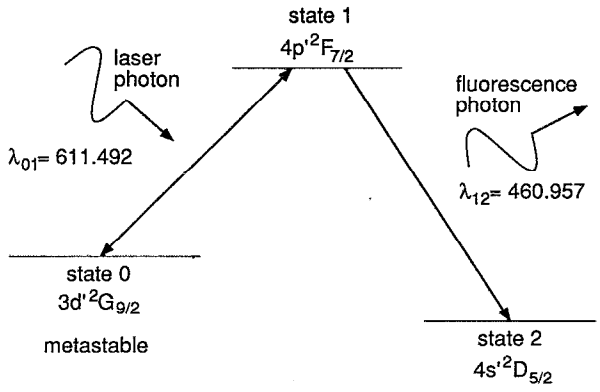

FIG. 4. Laser-induced fluorescence process. Laser photons pump the ions from state 0 to state 1 on the 611.492 nm spectral line. Spontaneous decay from state 1 to state 2 produces the fluorescence signal at 460.957 nm.

HD-SLM) with a narrow bandwidth of only 400 MHz and a pulse rate of 10 Hz. This laser was configured as a longitudinally pumped Littman-style oscillator,[20] followed by two transversely pumped amplifiers. The oscillator was operated in a single longitudinal mode. Its output had a Gaussian transverse spatial profile,[20] but the amplifiers convert this into a tear-drop shape. We observed this tear-drop profile qualitatively, using burn paper, but did not characterize it further.

To adjust the beam intensity without affecting the laser operation, we inserted neutral-density optical filters in the beam path between the laser and the plasma chamber. They did not noticeably alter the spatial profile of the beam. To further reduce the intensity, the beam was expanded to an area of 0.5 cm^2.

A portion of the beam was split off to measure the pulse energy. We corrected the reading of the Joule meter (Molectron J3-09) for the optical attenuation of the windows and mirrors. To convert from pulse energy to intensity, we assume that the temporal waveform was rectangular with a duration of 2.5 ns, which is consistent with the 400 MHz bandwidth of the laser.

The beam was directed through the center of the discharge, and fluorescence was collected at an angle of 90°. The detection optics consisted of a lens, a slit, an 0.51 nm bandpass filter, and a photomultiplier tube (PMT). The slit was positioned in front of the PMT to image a 0.5-cm-long section of the laser beam, in the center of the plasma. We did not calibrate the detection sensitivity, so the signal intensities reported below are in arbitrary units. To improve the signal-to-noise ratio, the fluorescence signal was averaged over 20 pulses. Further details of the optical system and signal processing scheme are found in Ref. 4.

B. Results

To experimentally observe saturation broadening, we measured the spectral line shape for a series of laser intensities, as shown in Fig. 5. For each of these line shapes, we performed a numerical fit to a bi-Maxwellian curve. This fit yields two useful parameters: the spectral line width,

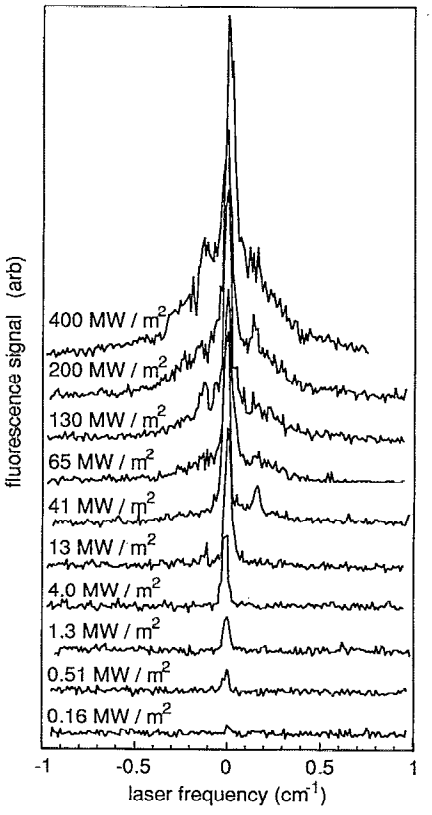

FIG. 5. Measured spectral line shape as function of laser intensity. Note that the line broadens at high laser intensities.

$\Delta\nu_{FWHM}$, and the fluorescence signal at the peak of the spectral line, referred to hereafter as the maximum fluorescence signal.

The results for signal strength versus laser intensity are presented in Fig. 6(a). As expected, the signal is linear at low intensities and saturates at high intensities. For our experimental setup, the onset of saturation, as defined in Ref. 11, is found at an intensity of about 10^7 W/m^2.

Figure 6(b) shows the linewidth $\Delta\nu_{FWHM}$ as a function of laser intensity. The spectral line is narrowest at low laser intensities, and it depends very little on the intensity below the saturation level of 10^7 W/m^2. At higher intensities, saturation broadening is obvious; the linewidth increases with intensity. At the highest intensity employed, 3×10^8 W/m^2, saturation broadening is so severe that the ion temperature predicted by Eq. (2) would be four times the correct value.

In Fig. 6(c) we have combined the data of (a) and (b) to show $\Delta\nu_{FWHM}$ as a function of the maximum fluorescence signal. This confirms that broadening of the spectral line occurs when the transition is saturated.

One important aspect of saturation broadening that we did not examine experimentally is the influence of the spatial profile of the laser beam. The spatial profile will depend on a number of experimental conditions, such as, the configuration of the laser system, how the laser is aligned by the operator, and the type and quality of the optics associated with the experiment. Because of the many variables associated with the spatial profile, we choose to examine its importance by using a simulation of the LIF process.

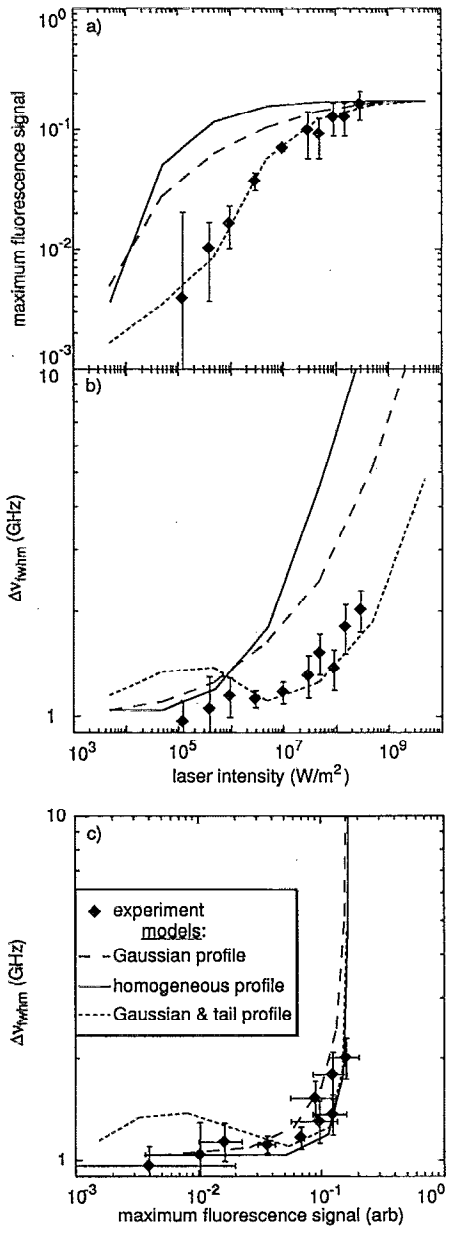

FIG. 6. Saturation broadening results from experiment (◆) and simulation (—). (a) Signal strength on the peak of the spectral line, as a function of laser intensity. (b) Linewidth $\Delta\nu_{FWHM}$ as a function of laser intensity. (c) $\Delta\nu_{FWHM}$ as a function of the signal strength. Both (a) and (b) are plotted on log-log graphs. Part (c) clearly shows that broadening of the spectral line occurs when the transition is saturated, and is almost independent of the spatial profile of the laser beam. The maximum signal from the simulation was scaled to represent the fraction of ions starting in state 0 and making the $0\rightarrow1\rightarrow2$ transition. The maximum signal of the experimental data was scaled to match the results of the simulation at high intensity.

III. SIMULATION

To simulate the saturation broadening process, we used the semiclassical atomic physics method of Goeckner and Goree.[11] Three electronically excited states of the ion, shown in Fig. 4, are accounted for. Transition rates are computed for three processes: absorption, stimulated emission, and spontaneous emission. Equation (6) of Ref. 11 is solved, yielding a prediction of the number of fluorescence photons N_{obs} that will be observed for a given laser wavelength, intensity, and bandwidth. Repeating this calculation for a series of central laser frequencies yields a predicted spectral line shape.

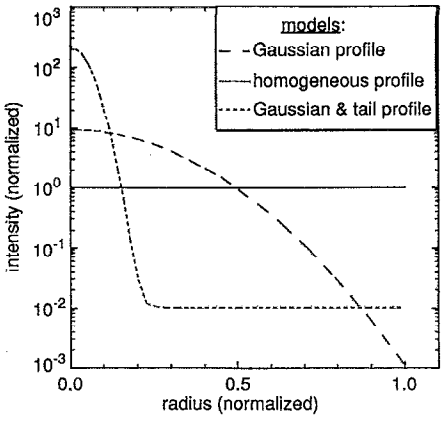

FIG. 7. Radial profiles of the laser beam intensity used in the semiclassical simulation. For the Gaussian profile with a homogeneous wing, the wing represents 1% of the total beam energy. To reveal these weak wings, we have plotted the profiles using semilogarithmic axes. The intensity is normalized for each profile so that the area-weighted integral under the intensity curve is 1.

The code makes the following assumptions. The electronic transitions are characterized by a Lorentzian absorption probability. The laser has a Gaussian laser frequency spectrum and rectangular temporal laser pulse waveform. The plasma ions have a Maxwellian ion velocity distribution. In running the code, we used the following input parameters, chosen to be consistent with the experiment: 400 MHz laser bandwidth, 2.5 ns pulse duration, and room-temperature (0.025 eV) ions.

The code also requires, as an input, the laser beam's transverse laser profile. This is important because saturation will first occur in the bright central part of a laser beam. At higher laser intensities, more of the beam's profile will be in saturation. Saturation broadening will thus depend on the profile shape, as shown earlier by Camparo.[18] We ran the simulation for three idealized intensity profiles. If the beam is axisymmetric, they can be described as (1) Gaussian profile, (2) homogeneous profile, (3) Gaussian profile with homogeneous wings. These model profiles are plotted in Fig. 7, where the area-weighted integral under the intensity curve are normalized to 1. In case (3), the wings represent 1% of the total beam energy; this was constructed so that the results fit the experimental data. However, it does not necessarily accurately represent the actual experimental spatial profile, which we did not measure. While we have described the model profiles as if they are axisymmetric, our results are still useful for nonaxisymmetric beams. Whether the spatial profile is peaked in the center or off center does not matter. What matters is the real distribution of intensity: how many square millimeters at one intensity, and how many at another.

Simulation results are compared to the experimental data in Fig. 6. The three spatial profile models yield qualitatively the same intensity dependence as observed in the experiment. Quantitatively, however, there are major differences. The homogeneous profile (1) predicts that satu-

ration begins[11] around 10^5 W/m^2, while in the experiment it begins near 10^7 W/m^2.

The simulation results for the three profile models differ greatly from one another in Figs. 6(a) and 6(b). This illustrates how saturation broadening depends on the spatial profile of the laser beam. Fortunately, however, the simulation results are insensitive to the spatial profile when they are plotted as linewidth versus maximum fluorescence signal, in Fig. 6(c). In this graph not only do the three simulations agree with one another, they also agree with the experimental data. Thus, it appears as if Fig. 6(c) might provide a universal curve for saturation broadening that is insensitive to the spatial profile.

IV. OPTIMIZATION METHODS

Three different methods were proposed in Ref. 11 for optimizing the laser intensity. Any of the three could be used by the experimenter to adjust the laser power to achieve minimal saturation broadening at the least possible sacrifice in LIF signal strength. The first method is to find the intensity at which the slope of the log-log curve shown in Fig. 6(b) is 0.015. The second method requires finding the asymptotic regions of the maximum signal at both high and low intensities. The optimum laser intensity is half the intensity at which the asymptotes intersect. The third method is to lower the laser intensity until the fluorescence signal at the peak of the spectral line is reduced 80%.

We have tested these three methods using the experimental data presented in Sec. II B. We found that the optimum intensity predicted by these methods were, respectively, 5×10^6, 8×10^6, and 3×10^7 W/m^2. These values are all comparable.

We recommend the third method of optimizing the laser intensity as the best, for the following reasons. First, the procedure is easy: the experimenter tunes the laser to yield the maximum signal, plots signal strength versus laser intensity to identify the saturation level, and then adjusts the laser to operate at 20% of this level. Second, it is the least sensitive to the spatial profile, as shown by the apparent universality of the curve in Fig. 6(c). Third, it does not require detecting weak signals at low laser intensities, as the first two methods do. Weak signals are more sensitive to noise, unless the experimenter spends time performing more signal averaging. We found that the third method of determining the optimal laser intensity assures a desirable line shape with only minimal broadening in all the cases we examined, both experimental and theoretical. From our results, we recommend the following procedure: tune the laser to yield the maximum signal, plot the signal strength versus laser intensity to identify the saturation level, and then adjust the laser to operate at 20% of this level.

ACKNOWLEDGMENT

This work was funded by the Iowa Department of Economic Development.

[1] R. Koslover and R. McWilliams, Rev. Sci. Instrum. **57**, 2441 (1986).
[2] F. Anderegg, R. A. Stern, F. Skiff, B. A. Hammel, M. Q. Tran, P. J. Paris, and P. Kohler, Phys. Rev. Lett. **57**, 329 (1986).
[3] M. J. Goeckner, J. Goree, and T. E. Sheridan, J. Vac. Sci. Technol. A **8**, 3920 (1990).
[4] M. J. Goeckner, J. Goree, and T. E. Sheridan, Phys. Fluids B **3**, 2913 (1991).
[5] R. A. Gottscho and T. A. Miller, Pure Appl. Chem. **56**, 189 (1984).
[6] E. A. Den Hartog, T. R. O'Brian, and J. E. Lawler, Phys. Rev. Lett. **62**, 1500 (1989).
[7] R. A. Stern, D. N. Hill, and N. Rynn, Phys. Lett. A **93**, 127 (1983).
[8] R. McWilliams and M. Okubo, Phys. Fluids **30**, 2849 (1987).
[9] F. Skiff and F. Anderegg, Phys. Rev. Lett. **59**, 896 (1987).
[10] R. A. Stern, Rev. Sci. Instrum. **56**, 1006 (1985).
[11] M. J. Goeckner and J. Goree, J. Vac. Sci. Technol. A **7**, 977 (1989).
[12] G. García and J. Campos, J. Quant. Spectrosc. Radiat. Transfer **34**, 85 (1985).
[13] H. R. Griem, *Spectral Line Broadening by Plasmas* (Academic, New York, 1974), p. 32.
[14] K. Miyamoto, *Plasma Physics for Nuclear Fusion* (MIT, Cambridge, MA, 1989), pp. 497–500.
[15] B. H. Bransden and C. J. Joachain, *Physics of Atoms and Molecules* (Longman, New York, 1983), pp. 207 and 229.
[16] M. J. Goeckner, J. Goree, and T. E. Sheridan, *Proceedings of the Fourth International Laser Science Conference, Atlanta, GA 2-6 October 1988* (American Institute of Physics, New York, 1989), pp. 761–766.
[17] D. N. Hill, Ph.D. thesis, Department of Physics, University of California, Irvine, CA, 1983.
[18] J. C. Camparo, Phys. Rev. A **39**, 69 (1989).
[19] R. Limpaecher and K. R. MacKenzie, Rev. Sci. Instrum. **44**, 726 (1973).
[20] M. G. Littman, Appl. Opt. **23**, 4465 (1984).